APPENDICES

APPENDIX A. MODEL DEVELOPMENT

This appendix provides supporting information for select components of the Coastal Systems Modeling Framework as described in the report *Partnership for Our Working Coast: A Community-Informed Transdisciplinary Approach to Maximizing Benefits of Dredged Sediment for Wetland Restoration Planning at Port Fourchon, Louisiana* (The Water Institute of The Gulf, 2022).

ACCRETION

The calculation for accretion rate at each wetland cell is fully described in the text, and is informed by data from Jankowski et. al (2017) and via personal communication from Gregg Snedden, USGS. The relevant data, from Coastwide Reference Monitoring System (CRMS) stations near to the project area, are shown in table form in Table A-1. The relationship between elevation and vertical accretion is shown in Figure A-1. These data justify the choice to use the elevation surplus / deficit framework to calculate accretion, and the choice to restrict accretion for higher elevation wetland cells.

Table A-1. Data from CRMS stations that was used to develop the conceptual framework for the accretion calculation. Accretion Surplus is defined as the local rate of RSLR subtracted from the Total Vertical Accretion rate. Stations with negative accretion surplus are vulnerable to drowning. Data points are from CRMS stations near Port Fourchon, shown in Figure 12 in the main text. Accretion rates for these stations were provided via personal communication from Gregg Snedden, USGS, and local rates of RSLR and station elevation are from Jankowski et. al (2017) in the main text. Accretion rates for these stations were provided via personal communication from Gregg Snedden, U.S.G.S., and local rates of RSLR and station elevation are from Jankowski et. al (2017).

CRMS Site	Wetland Type	Elevation Relative NAVD 88	Measured Accretion	Relative Sea-Level Rise Rate	Accretion Observation Time	Accretion Surplus/Deficit using Snedden Accretion
		(m)	(mm/yr)	(mm/yr)	(years)	(mm/yr)
164	Saline	0.1	12.0	9.9	12.3	2.1
175	Saline	0.1	7.9	4.5	9.9	3.4
178	Saline	0.2	12.1	7.0	9.6	5.1
292	Saline	0.2	15.3	11.8	10.8	3.5
310	Saline	0.0	14.3	7.3	11.9	7.0
318	Saline	0.0	14.3	10.7	9.6	3.6
337	Saline	0.1	9.7	10.8	9.6	-1.1
397	Brackish	0.0	11.3	14.0	12.0	-2.7
978	Saline	0.0	17.3	16.6	12.4	0.7

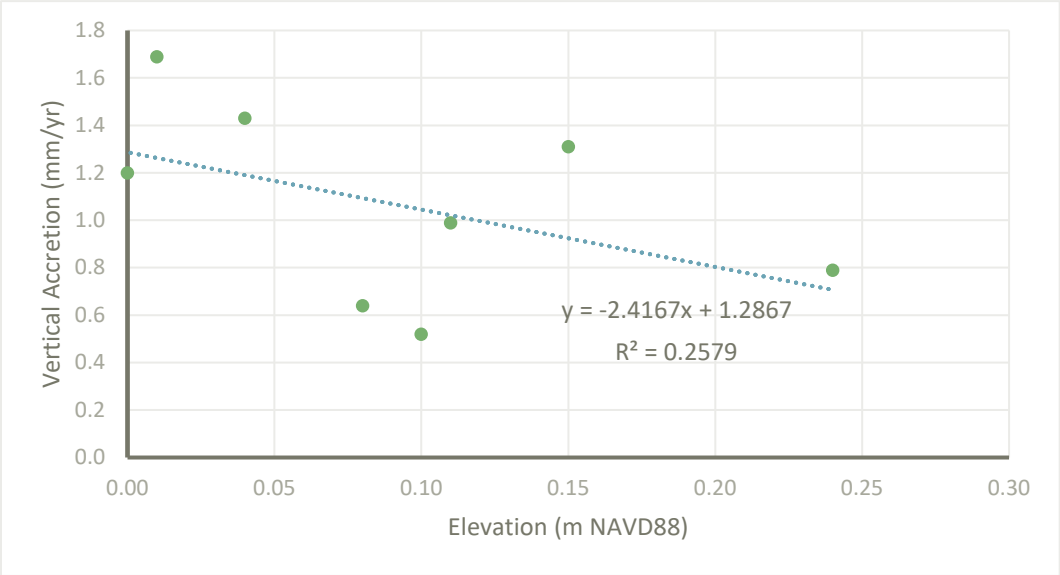

Figure A-1. Measured wetland accretion as a function of elevation at CRMS stations that are close to Port Fourchon. These data support the choice to lessen accretion rates for wetland cells at higher elevations.

EDGE EROSION

The Edge Erosion algorithm that was implemented in the Morphology Model converts the incident wave power at the wetland edge area to eroded wetland area using a wetland edge erodibility coefficient that was computed for Barataria Bay wetlands by Valentine and Mariotti (2019a). A description of how this calculation is implemented on the model grid is shown below for rectangular cells with geometry shown in Figure A-3, Figure A-4, and Figure A-5, with an adaptation to triangular cells shown in Figure A-6. This calculation is performed at every wetland edge in the model. An example is shown in Figure A-2

Because edge erosion is a slow process compared with the typical size of a model grid cell, a bookkeeping formulation of "ghost cells" are used to keep track of the amount of area within a cell that has eroded. The cell is considered to be fully lost only once 75% of the original area of the cell has eroded.

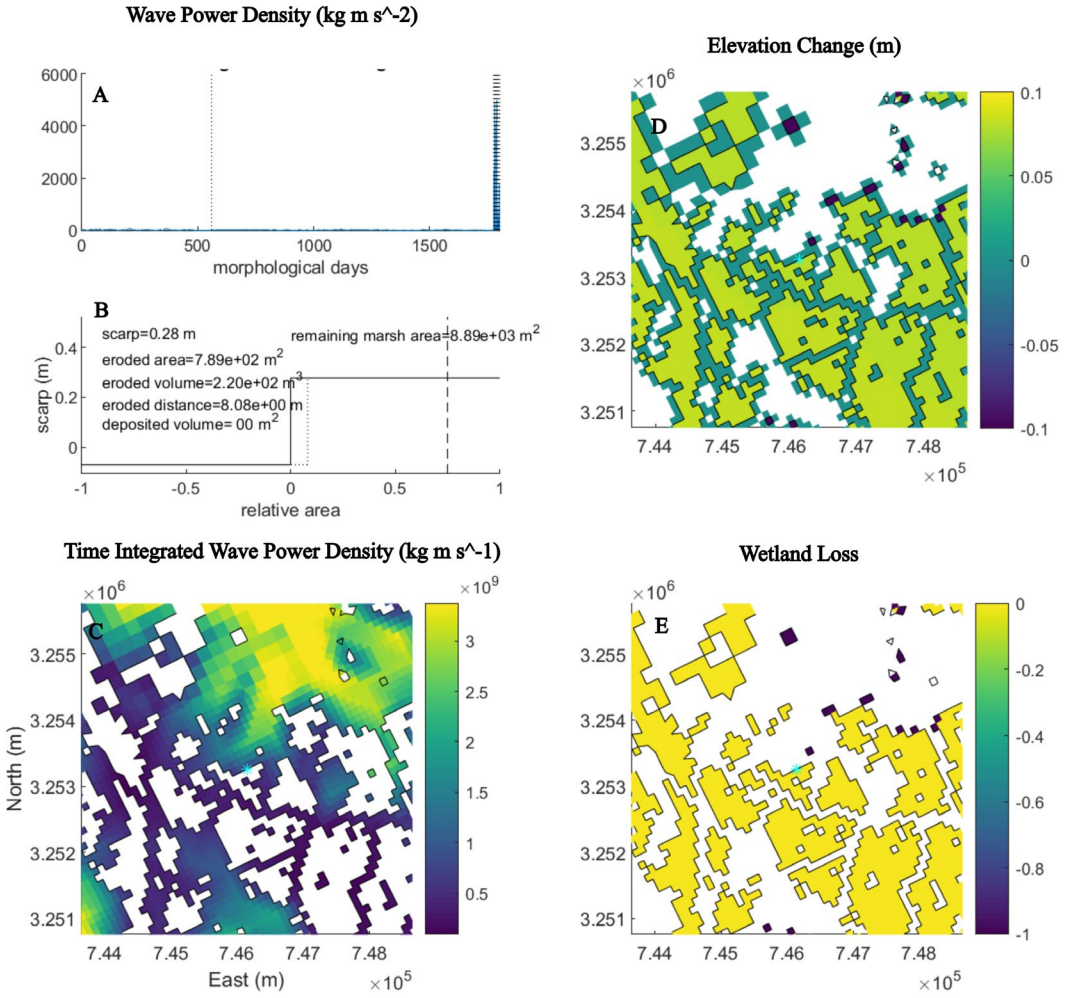

Figure A-2. Edge Erosion calculation at a single point in the model, indicated in figures by the cyan star. The timeseries of wave power density shown in A is used to calculate the erosion indicated in B. Eroded area, volume, and distance are all indicated in the figure. Deposited volume into the open water cell is zero, as all wetland erosion was assumed to be lost. The distance of the wetland retreat is shown by the thin dotted line and the threshold for final erosion of the wetland cell is shown in the heavy dotted line. A map of time integrated wave power density is shown for the surrounding area in C, and the overall change in elevation is shown in D. Wetland loss is shown in E, where loss is indicated by values of -1.

Definitions

The definitions for the parameters in the equations used to describe the edge erosion are listed here.

P Wave power vector at adjacent cell

P_i Wave power component entering cell

P_i' Wave power component entering cell, transformed across width of ghost cell

a_w Width of the ghost cell on the West side of Cell C. This is the distance by which the marsh has eroded back from the boundary between Cells W and C. Ghost cells along other edges will be indicated by the subscripts W, S, and E.

b_w Length of ghost cell on the West side of Cell C. This is the size of the cell edge minus any ghost cells that maybe encroaching from the North or South. In this example cells N and S are land, so $b_W = c_W$. But in the general case $b_W = c_W - (a_N + a_S)$.

c_W Length of cell edge between Cells C and W.

A_W Area of cell W

A_C Area of cell C

$A_{C,W}$ Area of western ghost cell within cell C. $A_{C,W} = a_W \cdot b_W$

R Volume of marsh eroded due to incoming wave energy.

α erodibility parameter.

δ Amount by which to increase elevation of cell W when redistributing eroded material.

G Volume of eroded material in cell C. This is the sum of all ghost cells.

S Scarp height. Calculated as the elevation difference between cells C and W.

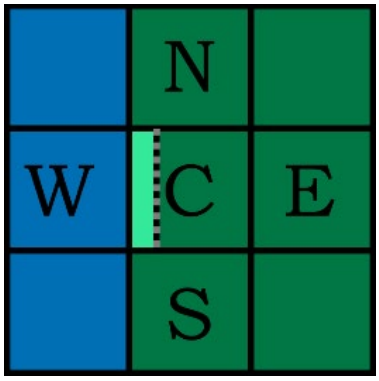

Figure A-3. Map view of cells relevant to the edge erosion module. Letters represent Central cell and the four cardinal directions. The "Ghost" cell is the area that has eroded away and is shown in a lighter color of green.

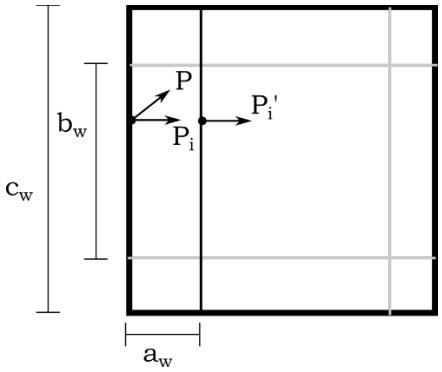

Figure A-4 . Blow up of cell C showing ghost cell dimensions and vectors for incoming wave energy transformation. Figure focuses on Western ghost cell w, but other ones are shown in light grey lines.

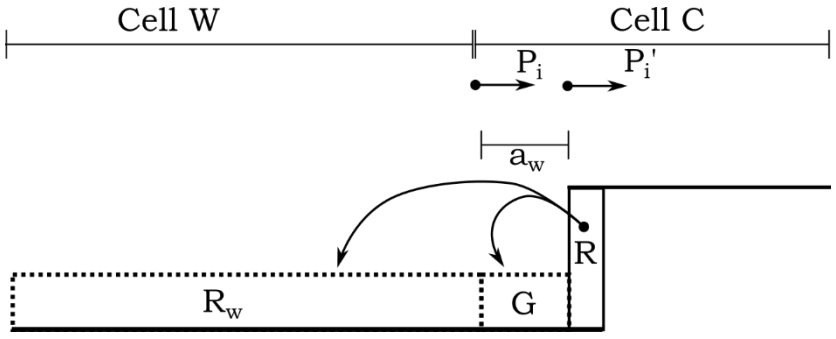

Figure A-5. Elevation view of cells W and C, showing dimensions of marsh eroded and deposited.

Assumptions

- All material that is eroded can be distributed in any proportion desired to the open water cell or to the wetland surface. In our model runs however, all material is assumed to be lost. This choice is due to data limitations in tracking eroded wetland material. The full functionality to distribute sediment is available in the code.

The relevant elevation for the P_i → P_i' transformation is that of the adjacent cell (cell W).

Algorithm Steps

1) Identify each cell face that is adjacent to non-vegetated cell (thus defining the marsh edge).

   Using SWAN output, calculate P_i at the cell face by computing the vector component of P that is normal to the wetland edge. If is desired that P_i and P_i' differ, an additional transformation can be performed at the corresponding ghost cell face.

2) Calculate the eroded volume using the proportionality constant identified by Valentine and Mariotti (2019b) to relate incident wave power and eroded volume. The power density (wave power per unit length of shoreline) is extracted directly from SWAN output.

   The volume eroded from the western face of Cell C as defined in Figure A-3 and Figure A-4; face is $R = \alpha P_i^{'} b_W$.

3) Distribute eroded volume between the adjacent cell and the eroding cell according to the area of the adjacent cell and that of the relevant ghost cell. So, the volume that moves to the adjacent cell is given by $R_W = R \cdot \frac{A_W}{A_W + A_{C,W}}$, and the elevation of the adjacent cell is increased by $\delta = \frac{R}{A_w + ac}$. The remaining volume is stored in the ghost cell $G_i = G_{i-1} + (R - R_W)$.

4) Update ghost cell properties:
   $a_{W,i+1} = a_{W,i} + \frac{R}{bS}$

5) After the full process (wave transformation, erosion, sediment redistribution) has taken place at each face in a cell, update the widths of the ghost cells. In a rectangular cell this would be $b_{i+1} = C - (a_n + a_s)$. See below for calculation within triangular cells.

If the cell is completely eroded (i.e. $a_W + a_E \geq c_S$ OR $a_N + a_S \geq c_W$) then the volume stored in the ghost cells ($\sum_{faces} G$) is distributed to that cell (unless sediment is considered to be low). It will leave an unvegetated bump exposed to wave action.

Triangular Cell Calculations

This calculation shows how to calculate the linear retreat rate and ghost cell calculations for a triangular cell.

t altitude of triangle to the face that is being eroded

t' altitude after erosion of area R has occurred

R Volume of marsh eroded due to incoming wave energy.

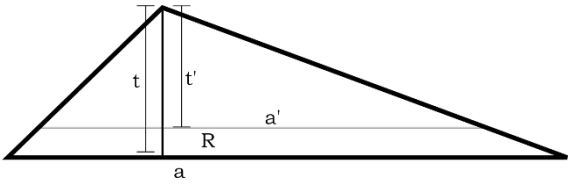

Figure A-6. Linear retreat rate calculated for triangular cell.

By similarity, t' can be stated in terms of a, a', and t.

$$t' = a' \frac{t}{a} \tag{0.1}$$

By the formula for the area of a trapezoid it can be said

$$R = \left(\frac{a + a'}{2} \right)(t - t') = \left(\frac{a + a'}{2} \right)\left(t - \frac{t}{a} a' \right) . \tag{0.2}$$

Solving for a' it can be seen that

$$a' = +\sqrt{\frac{a}{t}(at - 2R)} . \tag{0.3}$$

This is defined when $R \leq \frac{at}{2}$, which makes sense because $\frac{at}{2}$ is the area of the full triangle.

Thus for a triangular cell of known dimensions, experiencing a volume of marsh edge retreat R we can use equation (0.3) to find a' and equation (0.1) to determine t' and thus find the linear retreat distance.

METEOROLOGICAL INPUTS

As described in the main report, three separate classes of meteorological input conditions were used in the Morphology Model. These are quiescent conditions, cold front conditions, and tropical storm conditions. The process by which these three were amalgamated into an input time series is described in the main report, as was the selection process to determine which cold fronts to include. Below is described the technique that was used to make a continuous record from the North American Mesoscale Forecast System (NAM), as well as additional information on how the quiescent and tropical cyclone periods were developed.

Creating a Continuous, Spatially Varying Wind Forcing record

Output from the North American Mesoscale Forecast System (NAM) was combined with data from the Grand Isle gauge to obtain spatially variable wind forcings for quiescent and cold front periods. The combination is necessary because NAM output is available on a 6-hourly basis and therefore misses some velocity peaks, but while the data from the Grand Isle gauge does have sufficient temporal resolution (20 min) to capture those peaks it is, by definition, not spatially variable. The combination procedure is as follows.

The ratio between the Grand Isle wind record at hour 0, 6, 12, and 18 with each hour in between was used to create a multiplier to be applied to the NAM data at hour 0, 6, 12, and 18. For example, at hour 1, the ratio between the Grand Isle data at hour 0 and hour 1 was applied to the NAM data at hour 0 to create a wind record at hour 1. The data at Grand Isle at hour 0 is the reference hour. At hour 2 the ratio between the Grand Isle wind gauge at hour 0 and hour 2 is applied to the NAM data at hour 0 to create the wind at hour 2. This is repeated until hour 6 when the Grand Isle and NAM data at hour 0 is replaced by the data at hour 6; hour 6 becomes the reference hour. Ratios are calculated for each hour in the same way, updating the reference hour at hour 0, 6, 12, and 18.

Quiescent Periods

As described in the main report, cold fronts were identified in the pressure and temperature records obtained from the Grand Isle meteorological station. These data are provided at 20-minute temporal resolution and were averaged to hourly data.

This data was also used to develop wind forcings for quiescent periods following the method of Cobell et al. (2020). Each year was separated into the cold front season (October through March) and quiescent season (April through September). A statistical analysis was then performed on the quiescent season data to find a 28-day period within the record that best represented the average wind conditions and seasonal wind pattern mean of the entire data record.

First, a wind density function was calculated according to the method of Siegismund and Schrum (2001). This function combines the frequency of occurrence and mean wind speed for a given direction. Then an average cumulative distribution function (CDF) for the entire record was computed from the wind density function. The average CDF was compared to the CDF calculated for a moving window of 28 days. The magnitude of the different between the two CDF's was used to rank the periods. The period with the

smallest difference (August 3, 2015 through August 31, 2015) was used to represent the quiescent periods in the model.

Tropical Cyclone Selection

A realistic 30-year sequence of synthetic tropical storm events was generated to provide input conditions to the Morphology Model. This sequence was created using the same methodology as in the Louisiana Coastal Master Plan (CMP), and includes storms of varying intensity, frequency, and distance to the study area (Coastal Protection and Restoration Authority of Louisiana, 2017).

To save computational expense, an analysis was conducted to remove those storms that were unlikely to impact or overtop the barrier islands, given that the most significant and long-lasting geomorphic changes are most likely associated with storms that overwash or inundate the islands (Sallenger Jr., 2000).

This analysis was conducted by comparing the total water level – i.e., the combined contribution of wave run-up and storm surge – to a benchmark representing the berm and dune maximum elevation, following a similar methodology as presented in Long et al. (2020). Total water level was calculated by adding the storm surge to the 2% probability of wave runup exceedance calculated using the Stockdon empirical formulation, which requires significant wave height and wave period at 20 m depth offshore along with beach slope (Stockdon et al., 2006). Significant wave height, wave period, and storm surge were extracted for each of the synthetic storms from the ADvanced CIRCulation model (ADCIRC) output at two locations offshore of Port Fourchon at 28.867° N, 90.483° W and at 29.101° N, 89.978° W. Beach slope was estimated by taking the mean slope of 30 beach profiles taken from the CMP barrier island digital elevation model (ICM-BI) (Dalyander et al., 2021) at approximately 50 m spacing along the Caminada Headland. Beach slopes were calculated from manual extraction of the location and elevation of the dune (or berm) toe and the shoreline; the mean slope for these profiles was calculated as 0.0389. A value of 2.0 m was chosen as the threshold for storm exceedance based on dune and berm elevations along the Caminada Headland. Storms with a TWL that was below this level for the two nearshore locations where waves and water levels were extracted were excluded from the sequence (predicted TWL for the two locations was similar and generally varied by less than 0.25 m). A total of 8 of the original 30 storms in the 30-year sequence were identified as following below this threshold and were excluded from the analysis, leaving a 27-storm sequence to be modeled within the framework.

Table A-2. 30-year tropical storm sequence including the synthetic storm ID, storm central pressure, significant wave height (Hs), peak wave period (Tp), water level (WSE), wind velocity (WVEL), and total water level (TWL). Oceanographic data and wind speed values are provided for two locations (ST1 and ST2). Storms that were omitted from the sequence based on the TWL threshold are blacked out in the table.

	Storm ID	Central Pressure	year	ST1 Hs (m)	ST1 Tp (s)	ST1 WSE (m)	ST1 WVEL (m/s)	ST1 TWL (m)	ST2 Hs (m)	ST2 Tp (s)	ST2 WSE (m)	ST2 WVEL (m/s)	ST2 TWL (m)
1	298	975.25	1970	5.26	15.2	0.66	17.40	2.90	5.72	15.3	0.71	20.87	3.07
2	523	975.25	1971	5.04	12.8	0.76	21.39	2.62	6.06	12.9	0.85	25.84	2.90
3	188	965.25	1971	5.12	15.6	0.78	21.42	3.05	4.91	16.1	0.93	23.56	3.24
4	170	925.25	1971	6.77	18.5	1.65	39.57	4.77	7.97	18.0	2.33	42.67	5.61
5	*415*	*1005.25*	*1971*	*1.71*	*7.6*	*0.50*	*9.65*	*1.13*	*1.81*	*7.5*	*0.50*	*10.68*	*1.15*
6	556	905.25	1971	5.69	11.7	0.64	20.33	2.44	5.56	11.1	0.60	19.28	2.28
7	81	955.25	1973	5.83	12.8	0.69	35.25	2.69	7.07	12.9	1.19	33.68	3.41
8	297	955.25	1974	5.75	16.0	0.78	23.91	3.26	6.58	15.4	0.89	26.91	3.43
9	*83*	*995.25*	*1974*	*2.71*	*10.8*	*0.71*	*14.34*	*1.86*	*3.12*	*6.5*	*0.78*	*16.68*	*1.52*
10	515	955.25	1975	6.29	14.0	1.23	31.53	3.51	7.27	14.3	1.59	36.93	4.08
11	639	875.25	1975	7.64	10.1	3.14	68.63	4.94	7.82	12.3	3.08	67.82	5.30
12	*531*	*995.25*	*1976*	*2.48*	*9.5*	*0.59*	*11.16*	*1.55*	*2.45*	*9.2*	*0.59*	*11.93*	*1.51*
13	*38*	*965.25*	*1977*	*3.30*	*7.1*	*0.41*	*21.00*	*1.24*	*3.67*	*7.9*	*0.43*	*26.12*	*1.41*
14	503	995.25	1977	5.44	10.7	0.70	20.09	2.32	5.26	10.3	0.62	18.55	2.15
15	592	985.25	1977	6.38	13.3	1.08	25.06	3.24	6.87	13.4	1.04	25.69	3.31
16	291	975.25	1978	3.90	12.1	0.51	18.53	2.05	5.58	12.0	0.67	29.84	2.50
17	510	995.25	1979	5.48	11.1	0.77	20.45	2.45	6.30	11.2	0.75	21.58	2.57
18	291	975.25	1979	3.90	12.1	0.51	18.53	2.05	5.58	12.0	0.67	29.84	2.49
19	528	935.25	1979	6.35	17.3	1.10	28.57	3.91	7.12	16.4	1.09	32.27	3.91
20	357	965.25	1982	5.52	12.9	0.76	18.52	2.73	5.37	13.5	0.68	16.89	2.70
21	102	955.25	1984	3.90	14.7	0.64	19.27	2.52	2.91	7.5	0.68	20.96	1.51
22	*256*	*975.25*	*1985*	*3.43*	*10.7*	*0.53*	*13.09*	*1.83*	*2.97*	*10.3*	*0.48*	*11.15*	*1.63*
23	584	985.25	1985	5.46	10.6	0.63	22.20	2.22	4.82	10.0	0.55	19.13	1.97
24	600	985.25	1986	5.06	11.4	0.77	21.80	2.43	5.96	11.6	0.86	24.83	2.69

	Storm ID	Central Pressure	year	ST1 Hs (m)	ST1 Tp (s)	ST1 WSE (m)	ST1 WVEL (m/s)	ST1 TWL (m)	ST2 Hs (m)	ST2 Tp (s)	ST2 WSE (m)	ST2 WVEL (m/s)	ST2 TWL (m)
25	*349*	*965.25*	*1987*	*4.12*	*10.6*	*0.62*	*14.92*	*2.01*	*3.85*	*10.7*	*0.59*	*13.86*	*1.94*
26	298	975.25	1988	5.26	15.2	0.66	17.40	2.90	5.72	15.3	0.71	20.88	3.07
27	*125*	*985.25*	*1989*	*2.89*	*10.1*	*0.59*	*12.09*	*1.70*	*2.67*	*10.8*	*0.55*	*11.13*	*1.69*
28	*30*	*965.25*	*1989*	*2.90*	*6.3*	*0.41*	*20.46*	*1.10*	*3.71*	*6.3*	*0.67*	*31.92*	*1.45*
29	508	955.25	1992	6.85	14.7	1.53	31.14	4.01	7.30	14.9	1.43	31.02	4.03
30	544	975.25	1995	5.42	16.2	0.65	12.40	3.08	5.73	16.1	0.65	13.14	3.14

Stormier Sequence for Less Optimistic Scenarios

To create a stormier sequence for the Less Optimistic scenarios, a new list of storms was created by removing storms with a lower TWL. Storms with a TWL below 2.5 m at both stations were removed from the sequence and replaced by a random draw from the remaining storms. Storms that had a TWL above 2.5 m at one station, but not both, were left in the sequence, but not included in the random draw.

Storms 4, 8,10,11, 15, 19 were used as the pool to randomly draw from to re-fill the sequence. These storms represent the highest TWLs of the remaining pool (>3 m).

Table A-3. 30-year tropical storm sequence including the synthetic storm ID, storm central pressure, significant wave height (Hs), peak wave period (Tp), water level (WSE), wind velocity (WVEL), and total water level (TWL). Oceanographic data and wind speed values are provided for two locations (ST1 and ST2). Gray rows were removed for the stormier sequence and replaced with blue rows.

	Storm ID	Central Pressure	year	ST1 Hs (m)	ST1 Tp (s)	ST1 WSE (m)	ST1 WVEL (m/s)	ST1 TWL (m)	ST2 Hs (m)	ST2 Tp (s)	ST2 WSE (m)	ST2 WVEL (m/s)	ST2 TWL (m)
1	298	975.25	1970	5.2637	15.1554	0.65839	17.4032	2.9033	5.7201	15.2494	0.71168	20.8736	3.0664
2	523	975.25	1971	5.0411	12.7949	0.75993	21.3878	2.6147	6.0631	12.9269	0.84839	25.8405	2.9035
3	188	965.25	1971	5.1184	15.5932	0.77558	21.4152	3.0532	4.9052	16.1085	0.9326	23.5618	3.236
4	170	925.25	1971	6.7746	18.5364	1.6518	39.5704	4.7668	7.9733	17.996	2.3305	42.6661	5.6114
5	*415*	*1005.25*	*1971*	*1.7066*	*7.5594*	*0.49547*	*9.6519*	*1.1331*	*1.812*	*7.4871*	*0.50155*	*10.6775*	*1.1523*
6	556	905.25	1971	5.6937	11.6608	0.63963	20.3253	2.4361	5.5585	11.0458	0.60339	19.2761	2.2848
11	639	875.25	1975	7.6385	10.0627	3.1403	68.6284	4.9359	7.8165	12.3306	3.0784	67.8217	5.3042
7	81	955.25	1973	5.8329	12.8617	0.68511	35.2516	2.6907	7.0658	12.9181	1.1927	33.6755	3.4098
8	297	955.25	1974	5.7491	15.97	0.78269	23.9058	3.255	6.5778	15.3663	0.88554	26.9072	3.43
9	*83*	*995.25*	*1974*	*2.707*	*10.7962*	*0.71368*	*14.3368*	*1.8605*	*3.1194*	*6.535*	*0.77925*	*16.6791*	*1.5245*
10	515	955.25	1975	6.292	14.0429	1.2314	31.5275	3.5057	7.2674	14.3177	1.585	36.9263	4.077
11	639	875.25	1975	7.6385	10.0627	3.1403	68.6284	4.9359	7.8165	12.3306	3.0784	67.8217	5.3042
12	*531*	*995.25*	*1976*	*2.4847*	*9.4548*	*0.58749*	*11.1642*	*1.5497*	*2.4523*	*9.1473*	*0.58564*	*11.928*	*1.5105*
13	*38*	*965.25*	*1977*	*3.2957*	*7.0797*	*0.40532*	*20.998*	*1.2351*	*3.6698*	*7.8873*	*0.43101*	*26.1149*	*1.4065*
14	503	995.25	1977	5.4433	10.695	0.70444	20.088	2.3155	5.262	10.3178	0.6185	18.5463	2.1466
4	170	925.25	1971	6.7746	18.5364	1.6518	39.5704	4.7668	7.9733	17.996	2.3305	42.6661	5.6114
15	592	985.25	1977	6.3784	13.2875	1.0775	25.0582	3.2442	6.8716	13.4536	1.037	25.6865	3.314
16	291	975.25	1978	3.8968	12.091	0.51105	18.5318	2.0521	5.5787	11.9771	0.66814	29.839	2.4946
11	639	875.25	1975	7.6385	10.0627	3.1403	68.6284	4.9359	7.8165	12.3306	3.0784	67.8217	5.3042
17	510	995.25	1979	5.4836	11.0577	0.77382	20.4541	2.4456	6.2996	11.2367	0.74735	21.5785	2.5683
18	291	975.25	1979	3.8968	12.091	0.51105	18.5318	2.0521	5.5787	11.9771	0.66814	29.839	2.4946
8	297	955.25	1974	5.7491	15.97	0.78269	23.9058	3.255	6.5778	15.3663	0.88554	26.9072	3.43
19	528	935.25	1979	6.3539	17.2541	1.1047	28.5679	3.9128	7.1241	16.4	1.0851	32.2661	3.9112

	Storm ID	Central Pressure	year	ST1 Hs (m)	ST1 Tp (s)	ST1 WSE (m)	ST1 WVEL (m/s)	ST1 TWL (m)	ST2 Hs (m)	ST2 Tp (s)	ST2 WSE (m)	ST2 WVEL (m/s)	ST2 TWL (m)
20	357	965.25	1982	5.5239	12.931	0.76324	18.5172	2.7255	5.3707	13.4875	0.68399	16.889	2.7021
21	102	955.25	1984	3.897	14.7078	0.64258	19.2739	2.5172	2.9089	7.5434	0.68017	20.9575	1.5108
22	*256*	*975.25*	*1985*	*3.4258*	*10.74*	*0.53431*	*13.0896*	*1.8178*	*2.966*	*10.3001*	*0.48066*	*11.1479*	*1.6259*
23	584	985.25	1985	5.4557	10.5723	0.6258	22.2014	2.2202	4.818	9.9984	0.55129	19.1281	1.9682
8	297	955.25	1974	5.7491	15.97	0.78269	23.9058	3.255	6.5778	15.3663	0.88554	26.9072	3.43
24	600	985.25	1986	5.0648	11.4338	0.77338	21.7971	2.4347	5.9516	11.6119	0.86277	24.8287	2.6918
25	*349*	*965.25*	*1987*	*4.1232*	*10.567*	*0.62494*	*14.9248*	*2.0103*	*3.8538*	*10.6585*	*0.58868*	*13.8584*	*1.9396*
26	298	975.25	1988	5.2637	15.1554	0.65839	17.4032	2.9033	5.7201	15.2494	0.71168	20.8736	3.0664
27	*125*	*985.25*	*1989*	*2.8858*	*10.1001*	*0.59244*	*12.0854*	*1.7002*	*2.6694*	*10.7923*	*0.55186*	*11.1304*	*1.6903*
28	*30*	*965.25*	*1989*	*2.9009*	*6.2982*	*0.41014*	*20.4614*	*1.1027*	*3.7113*	*6.2942*	*0.66656*	*31.9151*	*1.4494*
29	508	955.25	1992	6.8516	14.7238	1.526	31.1428	4.0143	7.3011	14.9339	1.4253	31.0235	4.0306
30	544	975.25	1995	5.4226	16.1571	0.64714	12.4025	3.0763	5.7301	16.1173	0.64685	13.1435	3.1378

LITERATURE CITED

Coastal Protection and Restoration Authority of Louisiana. (2017). *Louisiana's Comprehensive Master Plan for a Sustainable Coast* (p. 184). Baton Rouge, Louisiana: Coastal Protection and Restoration Authority of Louisiana.

Cobell, Z., Sable, S., & Rose, K. A. (2020). *Calcasieu Ship Channel Salinity Control Measures Project (CS-0065): Larval Transport Modeling* (No. CS-0065) (p. 106). Baton Rouge, LA: The Water Institute of the Gul. Produced for and funded by the Coastal Protection and Restoration Authority.

Dalyander, P. S., Foster-Martinez, M., Di Leonardo, D. R., Georgiou, I., Miner, M., & Fitzpatrick, C. (2021). Barrier Island Tidal Inlet (BITI) Module and Barrier Island Digital Elevation Model (ICM-BI) Updates. Coastal Protection and Restoration Authority.

Jankowski, K. L., Törnqvist, T. E., & Fernandes, A. M. (2017). Vulnerability of Louisiana's coastal wetlands to present-day rates of relative sea-level rise. *Nature Communications*, *8*, 14792.

Long, J., Dalyander, P. S., Poff, M., Spears, B., Borne, B., Thompson, D., Mickey, R., Dartez, S., & Grandy, G. (2020). Event and decadal-scale modeling of barrier island restoration designs for decision support. *Shore & Beach*, 49–57.

Sallenger Jr., A. H. (2000). Storm impact scale for barrier islands. *Journal of Coastal Research*, *16*(3), 890–895.

Siegismund, F., & Schrum, C. (2001). Decadal changes in the wind forcing over the North Sea. *Climate Research*, *18*, 39–45.

Stockdon, H. F., Holman, R. A., Howd, P. A., & Sallenger, A. H. (2006). Empirical parameterization of setup, swash, and runup. *Coastal Engineering*, *53*(7), 573–588.

Valentine, K., & Mariotti, G. (2019a). Wind-driven water level fluctuations drive marsh edge erosion variability in microtidal coastal bays. *Continental Shelf Research*, *176*, 76–89.

Valentine, K., & Mariotti, G. (2019b). Wind-driven water level fluctuations drive marsh edge erosion variability in microtidal coastal bays. *Continental Shelf Research*, *176*, 76–89.